Bioinspiration & Biomimetics

PAPER

Bioinspired hierarchical impact tolerant materials

To cite this article: Susana Estrada *et al* 2020 *Bioinspir. Biomim.* **15** 046009

Bioinspiration & Biomimetics

RECEIVED
12 March 2020

REVISED
14 April 2020

ACCEPTED FOR PUBLICATION
29 April 2020

PUBLISHED
4 June 2020

PAPER

Bioinspired hierarchical impact tolerant materials

Susana Estrada[1], Juan Camilo Múnera[1], Javier Hernández[2], Mauricio Arroyave[2], Dwayne Arola[3,4] and Alex Ossa[1,5]

[1] Department of Production Engineering, Universidad EAFIT, Medellín, Colombia
[2] Department of Physical Engineering, Universidad EAFIT, Medellín, Colombia
[3] Department of Materials Science and Engineering, University of Washington, Seattle, WA, United States of America
[4] Department of Mechanical Engineering, University of Washington, Seattle, WA, United States of America
[5] Author to whom any correspondence should be addressed.

E-mail: eossa@eafit.edu.co

Keywords: bioinspiration, hierarchical structure, nano-reinforcement, energy absorption, nano-mineralization

Abstract

The quest for new light-weight materials with superior mechanical properties is a goal of materials scientists and engineers worldwide. A promising route in this pursuit is drawing inspiration from nature to design and develop materials with enhanced properties. By emulating the graded mineral content and hierarchical structure of fish scales of the *Arapaima gigas* from the nano to macro scales, we were able to develop bioinspired laminated composites with improved impact resistance. Activated by the addition of nano-particles of Al_2O_3 and nano-layers of TiN to a thermoplastic fiber substrate, new energy dissipation mechanisms operating at the nanoscale enhanced the energy absorption and stiffness of the bioinspired material. Remarkably, the newly developed materials are easily transferred to the industry with minimum associated manufacturing costs.

1. Introduction

Materials applications that demand resistance to impact loads, such as those present in aerospace structures, body armor, sports equipment, etc, fuel the constant search for stronger, tougher and increasingly lightweight materials. The ability to absorb impact energy requires strength, which is usually associated with materials that exhibit high density and brittleness. Similarly, impact tolerant applications require deformation ability to absorb and dissipate impact energy. These combination of properties (i.e., high strength and the capacity for large deformation) are typically challenging for engineering materials; however, can be widely found in biological materials [1–6]. After millions of years of evolution, biological materials have inspired engineers to develop novel materials with enhanced properties comprising a field of study known as biomimetics [7]. Bone, mollusk shells, osteoderms and fish scales are typical natural examples that have inspired engineers to develop new impact tolerant biomimetic materials with extraordinary properties [8–19].

Despite differences in structure and performance, biological materials share a commonality: they are made up of biopolymers and biominerals, which are organized hierarchically from the atomic to the macroscale [2, 3]. This structure is key to a combination of energy dissipation mechanisms that are activated over multiple orders of length scales [5]. Therefore, a recurring characteristic among impact tolerant bioinspired systems is the introduction of hierarchy at the micro and macroscales. Synthetic materials can be developed to achieve a hierarchical structure [20]. However, while biological materials generally exhibit between four and eight levels of hierarchy [1], man-made materials usually only reach up to three orders of hierarchy or less.

To exploit the possibilities of bioinspired hierarchical design Grunenfelder *et al* [12] manufactured carbon fiber reinforced epoxy composite laminates with a helicoidal arrangement of unidirectional plies, similar to the Bouligand structure of crustacean exoskeletons. Their laminates exhibited three orders of hierarchy through: (i) carbon fibers, (ii) the module of unidirectional fibers plied in a helicoidal pattern, and (iii) the repetition of that module along the cross-section of the laminate thickness. When compared to unidirectional and quasi-isotropic laminates, the helicoidal laminates showed a reduction in through-thickness damage. Cracks in carbon–epoxy composites extend preferentially through the matrix, rather than severing the strong fibers. The Bouligand-like stacking arrangement promoted

complex patterns of crack propagation, preventing catastrophic crack growth [12]. Other material systems emulating the protection systems of fish scales and mollusks have achieved two to three orders of hierarchy through: (i) the repeating stiff units (synthetic scale or nacre brick), (ii) the arrangement of stiff units emulating overlapping scales or nacre brick-and-mortar structure, and (iii) these arrangements attached to a polymeric substrate [9, 13, 14, 21]. In particular, Gu *et al* [14] fabricated a cross lamellar structure using additive manufacturing, which emulated the architecture of a conch shell. The addition of a second level of lamellar hierarchy increased the impact performance by 70% compared with a single addition of hierarchy level, and by 85% compared with the stiff material of the composite. Collectively, the results of these studies show that introducing additional orders of structural hierarchy can significantly improve the energy-absorbing capability of synthetic materials. While these studies help establish the promise of bioinspired concepts in materials development, the resulting arrangements achieved mostly by laser engraving and 3D printing have limited levels of hierarchy. This limitation, however, could be surpassed through the use of nanotechnology.

Besides energy dissipation, flexibility and lightweight are required characteristics in personal protection applications [6]. To this end, elasmoid scales emerge as proper natural models since they are lightweight mineralized units that enable mobility to fish while providing strong protection against predators. In particular, *Arapaima gigas* scales can provide protection against highly demanding predatory threats such as piranha attacks [22]. The structure of these scales consists of multiple layers of collagen fibers arranged in helicoidal arrangements with increased mineral content towards the outermost layers of the scale [22–27]. This work hypothesizes that this graded mineralization supported by a hierarchical structure is key to obtain enhanced protection without a significant increment of weight.

Using *A. gigas* fish scales as inspiration, here we incorporate nano-scale mineral reinforcements (e.g., Al_2O_3 and TiN) into laminar organic fibrous composites (UHMWPE) to develop a system that emulates the natural mineralization present in the scales. New orders of hierarchy are introduced within the structure of this impact tolerant system, which triggers new energy dissipation mechanisms at the nanoscale. Using this strategy, we developed a new generation of composites with five orders of hierarchy, which renders a considerable enhancement of energy absorption without a significant increase in weight.

2. Elasmoid fish scales

Elasmoid scales are flexible, lightweight, impact tolerant materials that help protect a wide variety of fish against predatory threats. They are mineralized units that are partially embedded within a highly flexible tissue backing layer, and overlap one another to maximize the capacity for protection [27–32]. Like other biological structural materials, elasmoid scales possess a hierarchical structure. They are comprised of a combination of type I collagen fibers and apatite, which are the fundamental constitutive elements among other natural mineralized systems [4]. The role of fibers and reinforcements in fish scale composites is the opposite of most mineralized biological tissues (e. g. dentin and bone), here the collagen fibers are the organic portion and the matrix (i.e. minerals) are the reinforcement. Depending on the degree of mineralization, elasmoid scales can be divided into two different layers (figure 1(a)): a highly mineralized rough external layer termed limiting layer (LL), consisting of a mineral matrix with randomly dispersed thin collagen fibers (30–50 nm in diameter), and a basal plate commonly regarded as the elasmodine, which consist of densely packed layers of unidirectional collagen fibrils (100–160 nm in diameter). Depending on the mineral distribution, the elasmodine can be further divided into the external (EE) and internal elasmodine (IE). The EE is more highly mineralized due to an increased reinforcement of apatite platelets [33]. Collagen fibrils of the elasmodine are packed into larger fibers, which are aligned and assembled into individual unidirectional plies (or lamellae). These plies are stacked with a helicoidal arrangement commonly known as a Bouligand structure [22].

Interestingly, the Bouligand structure serves a critical role in the mechanical behavior of this material system by enhancing the ductility and toughness of scales [34]. Furthermore, the hierarchical structure facilitates the dissipation of energy across different length scale levels [22, 35]. At the macroscale (>1 mm), the outer layer (LL) dissipates energy through mechanisms of brittle fracture, while the basal fibrous structure undergoes a high degree of deformation before failure [36]. At the micro-scale (1 μm to 1 mm), the Bouligand arrangement facilitates a reorientation of the lamellae in response to the loading direction. Under in-plane tensile loads, deformation occurs through a combination of stretching and interfacial sliding mechanisms [33, 34]. And at the nano-scale (1 nm to 1 μm), the collagen fibrils straighten, rotate, stretch, and eventually undergo fracture, a process that dissipates substantial energy. This process is accompanied by the resistance to sliding caused by the interfibrillar nanoscopic mineral platelets of apatite. As such, this behavior is highly dependent on the mineral content.

In mineralized tissues consisting of moderate mineral content, the collagen fibrils uncoil first and then increase their stiffness due to the stress transfer among the mineral platelets present [5]. At the

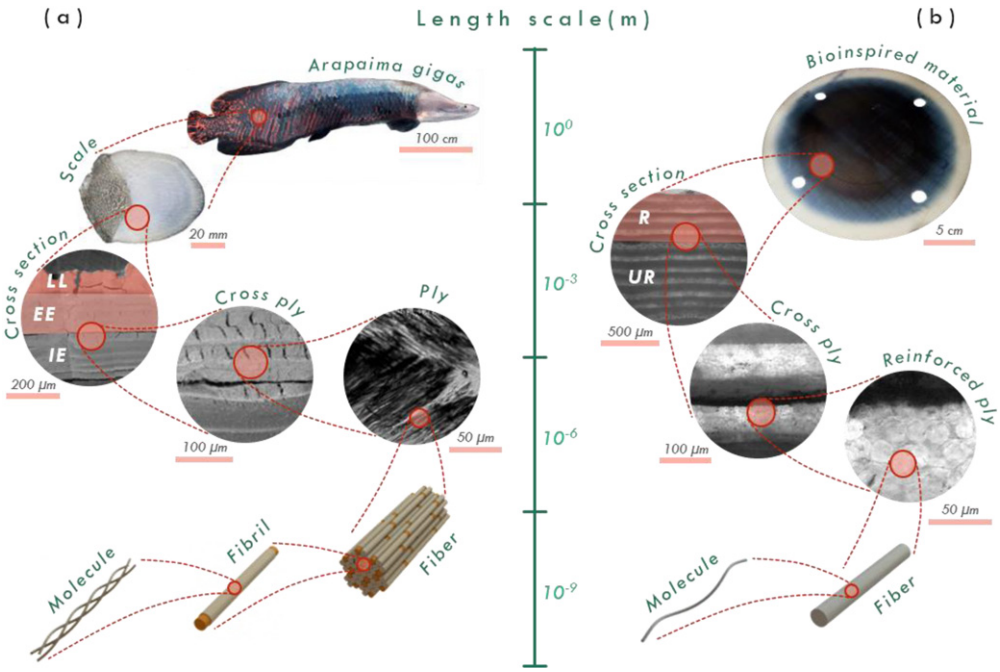

Figure 1. Hierarchical structure of *A. gigas* scales and bioinspired composites, from the macroscale (10^0 m) to the atomic scale (10^{-9} m). Coloring represents a higher degree of mineralization. (a) Hierarchical structure of arapaima scales, shown from top to bottom: *A. gigas* fish, an elasmoid scale, a cross-section of the scale, collagen fibers arranged in a cross-ply configuration, a ply of unidirectional fibers, a mineralized collagen fiber with colored dots representing hydroxyapatite, a mineralized collagen fibril with colored dots representing hydroxyapatite, and the tropocollagen structure of the collagen molecule. (b) Hierarchical structure of bioinspired composites, showing from top to bottom: a plate of bioinspired material, the cross-section of the laminate showing graded mineralization (R, Reinforced and UR, Un-reinforced), UHMWPE fibers arranged in a cross-ply configuration with a nano-mineralized layer, two plies of UHMWPE fibers reinforced with a layer of nano-mineralization, a UHMWPE fiber and, a UHMWPE molecule.

atomic scale (<1 nm), the collagen molecules dissipate energy by uncoiling and through breaking and reforming of hydrogen bonds between molecular chains [5]. This interplay between the different energy dissipation mechanisms allows efficient and light-weight protection against predation; however, these mechanisms are highly affected by the hydration level of the scales. Indeed, the stiffness, strength and toughness of the scales have shown to be highly dependent on water content [25, 37].

Arapaima fish possess elasmoid scales, providing protection against piranha attacks. The *A. gigas* is a species of arapaima that is native to the Amazon river basin of South America and is among the world's largest freshwater fish. It is covered by scales with lengths between 5–7 cm and average widths of ∼4 cm [25]. The LL of its scales is about 600 μm in thickness, while the elasmodine can be as thick as 1000 μm. Unlike most other fish, the lamellae of the elasmodine are arranged with a stacking sequence of approximately 0°/90°, which is equivalent to a cross-ply orthogonal laminate structure [33]. The ply thickness ranges from 30–60 μm [24, 33]. The constitutive fibers of each lamella have a diameter of approximately 1 μm and these in turn consist of a large number of fibrils of smaller diameter (∼100 nm) [24]. The mineral structure within the layer of these scales was recently detailed and consists of platelets with a thickness of ∼50 nm and diameters of ∼500 nm [22, 25]. Overall, the microstructure of the *A. gigas* scales exhibits six orders of hierarchy (figure 1(a)).

3. Materials and methods

Here we propose a material system inspired by the structure of *A. gigas* scales. The foundation is a laminated composite of unidirectional plies of ultra-high molecular weight polyethylene (UHMWPE) fibers within a rubber-based matrix. The laminate possesses a cross-ply arrangement similar to the 0°/90° ply configuration of arapaima scales [33]. These composites are widely used in the armor industry under brands such as Spectra® and Dyneema®. Analogous to the mineral reinforcement of scales, we introduce nano-scale mineral reinforcements between the exterior-most layers of the laminate to increase the strength and energy absorption, without significantly increasing the weight of the material. The structure of this newly constructed material exhibits principles that are consistent with those of the *A. gigas* scales (figure 1(b)).

The laminates were comprised of eight layers of Dyneema® HB50, consolidated into a plate by thermo-pressing. Selected properties of Dyneema® HB50 and Dyneema® fibers are shown in table 1. Each layer of Dyneema® HB50 consisted of four plies of unidirectional fibers cross-plied at 90° to each

Table 1. Selected properties of Dyneema HB50 and Dyneema fibers. Information obtained from suppliers' data sheets.

HB50	Dyneema fibers		
Areal density (g m^{-2})	Axial tensile modulus (GPa)	Transverse modulus (GPa)	Elongation at break (%)
226–240	52–132	3	3–4

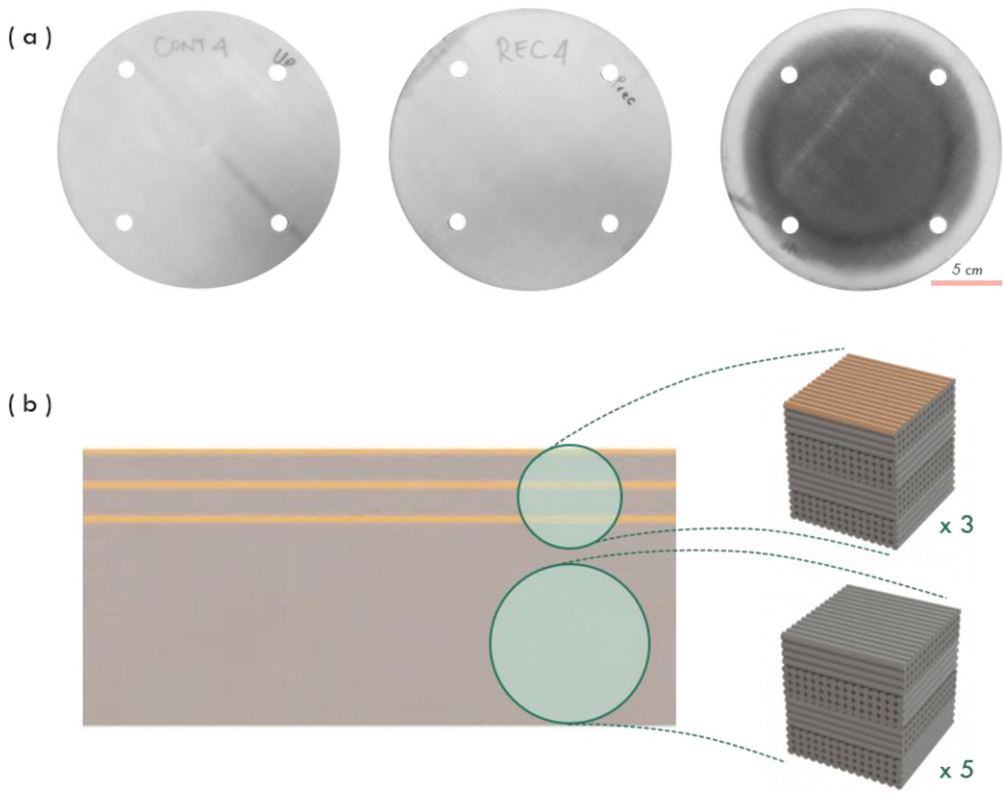

Figure 2. Bioinspired impact tolerant materials. (a) Pictures of bioinspired samples. Shown from left to right: unreinforced laminate, laminate reinforced with Al_2O_3 nanoparticles, and laminate reinforced with TiN nanocoatings. (b) Schematic mineral distribution of reinforced materials. Coloring represents mineralization. The three outermost layers of Dyneema® HB50 were reinforced with minerals (i.e., Al_2O_3 nanoparticles or TiN nanocoatings) while the five inner layers were unreinforced.

other. The laminates were pressed at 100 bar at a temperature of 125 °C for 35 min and then removed from pressure once the temperature was below 60 °C, following material's supplier recommendations. For repetition, five samples of each design were fabricated and tested.

To compare the mechanical performance and structural differences of the bioinspired materials, three different types of composites were fabricated: (i) unreinforced laminates of the UHMWPE composite, (ii) reinforced laminates with aluminium oxide (Al_2O_3) nanoparticles, and (iii) reinforced laminates with titanium nitride (TiN) nanocoatings. Each sample consisted of a disc-shaped plate with a 200 mm diameter and ∼2 mm of thickness (see figure 2(a)).

Two different manufacturing strategies were adopted to introduce the nano reinforcements into the laminates. A nano-spray process was used to deposit spherical nano-particles between the laminate plies, while radio frequency magnetron sputtering was used to introduce the nano-coatings.

3.1. Aluminium oxide reinforced laminates

The nano-spray process for introducing the Al_2O_3 nanoparticles reinforcement consisted of spraying three of the eight layers of the laminate with a colloidal suspension. These reinforced layers were stacked successively towards the external face of the laminate, combined with five non-reinforced layers, followed by thermo-pressing (see figure 2(b)). After thermo-pressing, the stacking sequence of the laminate exhibited two different regions along the cross-section, which resembled the elasmodine structure of arapaima scales. Specifically, the laminate consisted of a mineralized external region (i.e. EE), and a non-mineralized basal region (i.e. IE) [26].

In the manufacture of Al_2O_3 reinforced laminates, liquid polyurethane (PU) was mixed with Al_2O_3 nanoparticles (∼500 nm in diameter, MSESUPPLIES). The mixture was prepared in the following weight proportions: PU 41.7%, solvent 21%, catalyst 26.9% and Al_2O_3 particles 10.4%. The mixture of nanoparticles was applied by using a paint gun

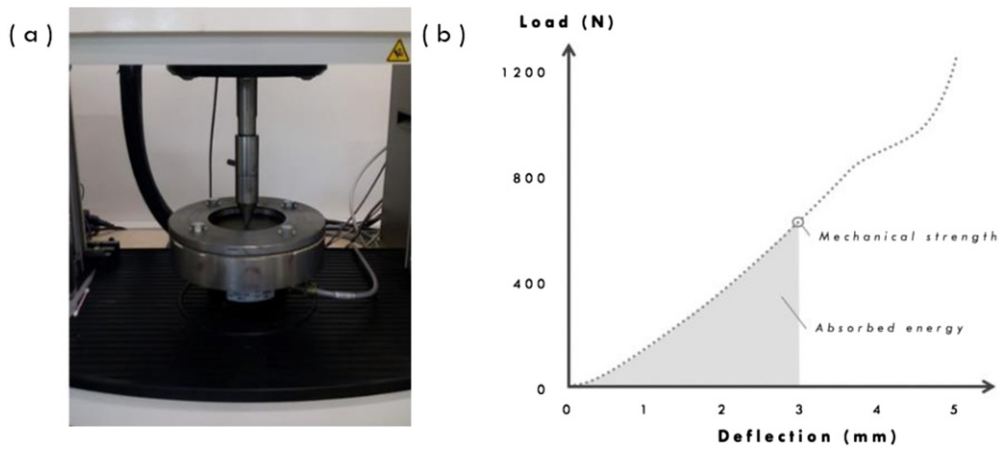

Figure 3. Impact test. (a) Impact test fixture showing clamping and striker. (b) Typical load-deflection response on an impact test. Mechanical strength is defined as the maximum impact load achieved at 3 mm of deflection, while energy absorption was defined as the area under the load-deflection curve from 0–3 mm of deflection.

in two layers of homogeneous thickness, reaching approximately 500 μm. Three of the eight layers forming the bioinspired laminate were coated with this mixture between 1 and 10 min after adding the catalyst. The coated layers were left to dry for 24 h at room temperature before consolidating into a laminate through thermo-pressing.

3.2. Titanium nitride reinforced laminates

Titanium nitride (TiN) layers were produced by a high vacuum radio frequency magnetron sputtering equipment (H2 Intecovamex) configured with a cubic stainless-steel vacuum chamber (300 × 300 × 300 mm). The distance substrate—target was 100 mm. High purity (99.995%) titanium discs were used as the magnetron-sputtering targets. The sputtering process was developed at 5 mTorr of pressure in atmosphere of argon (90%) and nitrogen (10%) during 70 min at 150 watts of radio frequency power.

To manufacture the TiN reinforced laminates the three outermost layers of the composite were coated before thermo-pressing with a thin layer of TiN (∼300 nm in thickness) using radio frequency magnetron sputtering. Thereafter, the reinforced and unreinforced layers were stacked and thermo-pressed with the same two-region configuration described for Al_2O_3 reinforced laminates (see figure 2(b)).

3.3. Impact tests

Impact tests were performed on the manufactured samples by using a fully instrumented TA Electro Force 3300 equipment with a loading rate of 2 m s^{-1}. A custom clamping was used to hold the laminates in place during impact, in which laminates were fixed through bolts, leaving 100 mm of free space for the laminate to deform. The clamping device was made of hardened steel (figure 3(a)). The steel striker was made with a conical-spherical shape to allow a considerable energy transfer to the laminates tested (figure 3(a)). The impact results were evaluated at 3 mm of deflection in all the tests to stay at a maximum of 0.5R of deformation, where R is the striker tip radius. Special care was taken to avoid any slip of the samples during testing by using sandpaper between samples and clamping device.

A typical load-deflection impact response is shown in figure 3(b). Mechanical strength was considered here as the maximum impact load at 3 mm of deflection, stiffness was defined as the ratio between load and deflection at 3 mm of deflection, and the energy absorbed was defined as the area under the load-deflection curve once achieved 3 mm of deflection, as shown in figure 3(b). The choice of 3 mm of displacement to evaluate the energy absorbed by the tested samples ensured to have a constant speed of the striker up to this point. Soon after 3 mm the striker started to decelerate, reducing the impact speed. Further, after approximately 1 mm of displacement the deformation of the samples showed permanent deformation (plasticity), which was important as a measure of the energy absorbed by the samples. It is worth noting that none of the samples tested reached failure.

3.4. Microscopy tests

Small sections of the bioinspired laminates (about 2 mm in thickness) were embedded in cold-cured epoxy resin in order to inspect their microscopic characteristics. These sections were further ground with sandpaper with successive grit sizes of 120, 220, 400, 600, 1000 and 1200, until having final thicknesses of the laminates of about 200 μm. Further polishing by means of red felt polishing cloths was performed using diamond particles of 6 μm, 3 μm, and 1 μm in size. Optical microscopy was then carried out on the samples using transmitted light by using an optical microscope (Axiovert 40 MAT, Carl Zeiss, NY). The same samples were further used for atomic force microscopy analysis. Images were

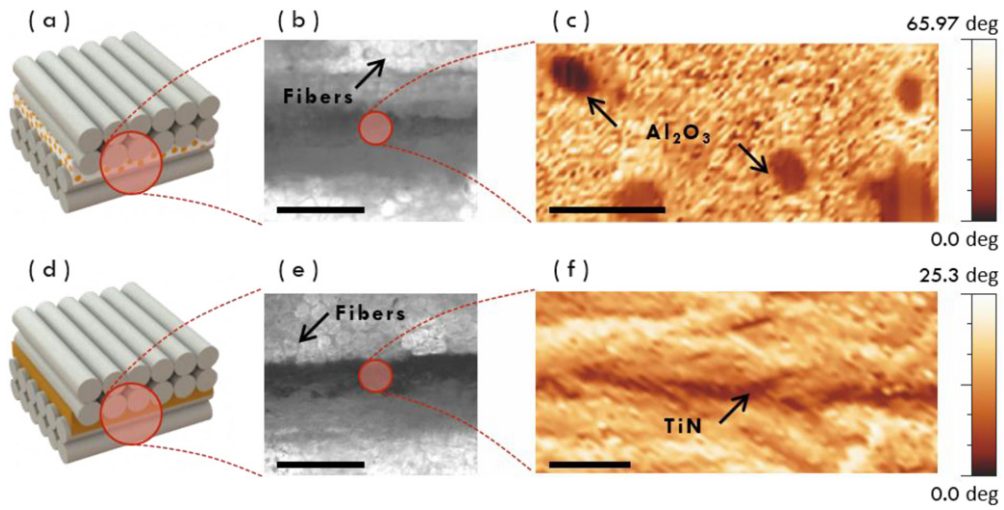

Figure 4. Micro and nanostructure of the bioinspired composites. (a) Scheme of cross-ply fibers reinforced with aluminium oxide (Al_2O_3) particles in a polyurethane matrix; (b) cross-section of a laminate reinforced with Al_2O_3 observed with optical microscopy using transmitted light, scale bar corresponds to 100 μm; (c) AFM non-contact phase image of a laminate reinforced with Al_2O_3 nanoparticles with a diameter of ~500 nm, scale bar corresponds to 1 μm, Al_2O_3 nanoparticles are pointed by arrows; (d) scheme of cross-ply fibers reinforced with titanium nitride (TiN); (e) cross-section of a laminate reinforced with TiN observed through optical microscopy using transmitted light, scale bar corresponds to 100 μm; (f) AFM non-contact phase image of a laminate reinforced with TiN showing a TiN layer of ~300 nm, scale bar corresponds to 1 μm, TiN layer is pointed by an arrow.

obtained at standard conditions (T = 20 °C and R.H. = 50%) using an atomic force microscope (AFM; XE7, Park Systems Inc.). Commercial silicon AFM tips with diamond-like carbon (DLC) coating (TAP150, budget sensors) having a nominal stiffness $k = 5$ N m^{-1} and tip radius $R = 25$ nm were used in the phase non-contact mode.

4. Results and discussion

One of the main differences between the two typologies of reinforced laminates manufactured was the continuity of the reinforcing phase. While the Al_2O_3 particles consisted of discrete particles dispersed in a polyurethane matrix, the TiN nano-reinforcement was configured in a continuous layer as shown schematically in figure 4. The dispersed reinforcement of Al_2O_3 is shown between the fiber plies in figure 4(a), and the continuous reinforcement of TiN is shown as a monolithic layer between fiber plies in figure 4(d). Both of the reinforced laminate configurations possess a five-order hierarchical structure as shown in figure 1(b).

4.1. Microscopy results

The microstructure of the bioinspired laminates is shown in Figures 4(b) and (e), with light and dark alternating regions representing layers of fibers arranged in a cross-ply configuration. The fibers oriented perpendicular to the observer can be seen in the lighter areas of the image, where circular individual UHMWPE fibers with a diameter of ~17 μm can be seen. The dark area towards the center of the images corresponds to one nano-mineralized layer. Figure 4(c) shows the structure of Al_2O_3 particles with diameters of ~500 nm dispersed in the polyurethane matrix, while figure 4(f) shows the TiN nano-layer with a thickness of ~300 nm.

4.2. Impact results

Results of the impact tests show that both the Al_2O_3 and TiN nano-scale reinforcements increased the impact resistance of the bioinspired composites (figure 5). While the unreinforced composites reached an average maximum load of approximately 640 N, the bioinspired composite reinforced with Al_2O_3 nano-particles reached an average maximum load of 730 N, representing over 14% increase in impact load. On the other hand, the nano-reinforced TiN composites achieved an average maximum load of 760 N, an increase of approximately 18% when compared with the unreinforced material.

The differences in resistance to transverse deformation of the reinforced composites under impact loading are also reflected in their ability to absorb impact energy. Figure 6 shows the absorbed energy profiles for the materials, with respect to their stiffness. While the unreinforced material reached an average absorbed energy of 0.80 J with stiffness of roughly 305 N mm^{-1}, the laminate reinforced with Al_2O_3 reached an average absorbed energy of 0.96 J with a stiffness of 335 N mm^{-1}. That represents a 20% increase in absorbed energy with a 9% increment of stiffness for the Al_2O_3 reinforced materials. On the other hand, the TiN-reinforced materials achieved a 0.98 J of absorbed energy with a stiffness of 355 N mm^{-1}. When compared to the unreinforced materials, that represents a 23% increase

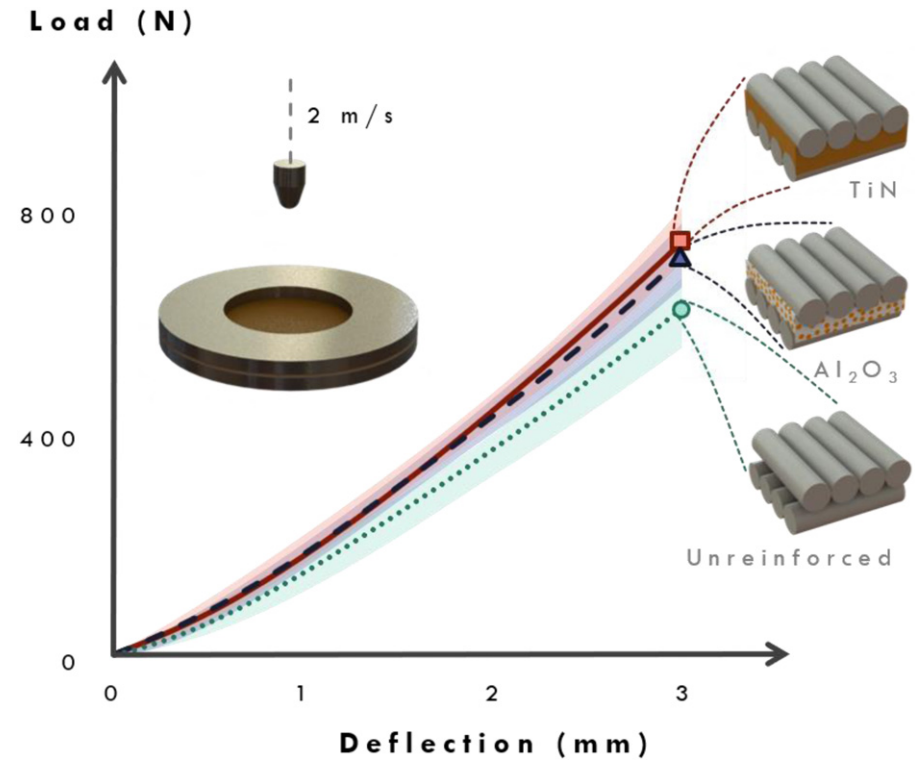

Figure 5. Load versus deflection response from the impact tests performed on the bioinspired and unreinforced materials. Colored areas with transparency represent the standard deviation of the measured responses for each type of material.

in energy absorbed and an 18% increment in stiffness. In demanding impact loading applications like aerospace, body armor and sports equipment, energy enhancements of these levels can render equivalent weight reductions. The statistical analyses showed that the differences in response between the three different composites were significant ($p \leqslant 0.05$). The post-hoc analysis showed that there were significant differences between the unreinforced and bioinspired composites, but no significant difference in performance between the Al_2O_3 and TiN reinforced composites (see table 2).

4.3. Discussion

The introduction of hierarchical structures has recently been used to obtain extraordinary properties in synthetic materials [14]. However, it is presently impossible to introduce hierarchy at length scales below the micro and macro scales by using technologies such as additive manufacturing or laser engraving. As such, nanotechnology appears to be the most viable option for introducing new levels of hierarchy in the development of synthetic materials. The bioinspired composites fabricated in this study achieve five orders of hierarchy: (i) the UHMWPE fibers; (ii) a ply of unidirectional fibers; (iii) a laminated layer of four cross-ply unidirectional plies; (iv) three nano mineralized layers; and finally (v) the bioinspired laminate with 'graded' mineralization, similar to the EE and IE of fish scales (figure 1). A sixth order of hierarchy could be achieved if the molecules of the polyethylene fibers were considered at the atomic scale.

Fish scales exhibit an interesting distribution of mineral content across their thickness. Arola *et al* studied the mineral content of the outermost layer of the scale (LL) in different fish species [36]. Regardless of species, the mineral content is maximum on the exterior surface of the LL, and then decreases to the LL/EE interface. The mineral content remains nearly constant in the EE and then undergoes an abrupt decrease to nearly zero in the IE. In essence, the IE consists of plies of unidirectional collagen fibers without any mineral content. For the arapaima scales, the volume fraction of apatite decreases from 60% to 40% over the thickness of the LL, remains nearly constant in the EE and then reduces to 0% within IE [36]. Similarly, our bioinspired materials have highest mineral content towards the external layers of the composite due to the TiN and Al_2O_3 reinforcement. The volume fraction decreases to 0% in the inner layers of the material, which mimics the distribution found in the EE and IE layers of elasmoid scales.

The mechanical properties of the bioinspired laminates are highly dependent on the properties of the reinforcement. The Young's modulus of Al_2O_3 and TiN is approximately 300 GPa and 600 GPa, respectively. Apart from Young's moduli, the difference in morphology between the two types of reinforcements is also important to the mechanical responses.

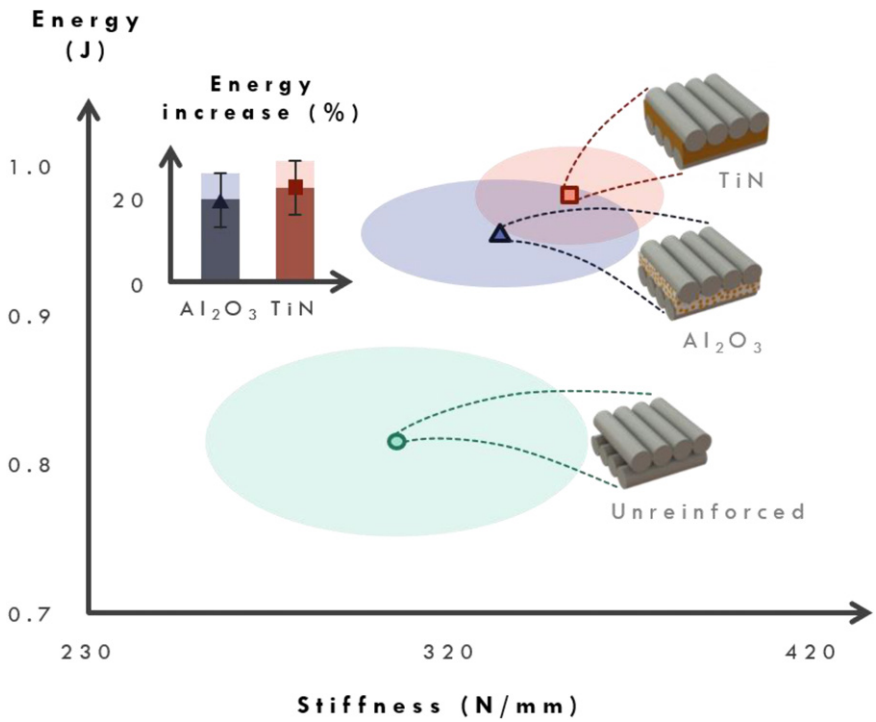

Figure 6. Absorbed energy versus stiffness of the bioinspired and unreinforced materials. The inset shows the percentage of energy increase of the reinforced materials (Al_2O_3 and TiN) in comparison to the unreinforced laminates. Colored areas with transparency represent the standard deviation of the measurements of each type of material.

Table 2. Dynamic testing results for reinforced and unreinforced samples, showing the mean (μ), standard deviation (σ), and coefficient of variation (CV) of the load, absorbed energy, and stiffness achieved by each sample configuration under impacts at 2 m s^{-1}. For repetition, five samples for each configuration were tested ($N = 5$).

Sample	Load (N)			Energy (mJ)			Stiffness (N mm^{-1})		
($N = 5$)	μ	σ	CV	μ	σ	CV	μ	σ	CV
Unreinforced	639.7	48.5	8%	0.796	0.049	6%	305.3	16.2	5%
Reinforced with Al_2O_3	729.6	49.5	7%	0.956	0.029	3%	333.9	16.5	5%
Reinforced with TiN	756.7	32.1	4%	0.982	0.032	3%	359.1	10.7	3%

The Al_2O_3 particles were dispersed within a rubber-based matrix, serving as discontinuous reinforcements, while the TiN coatings formed a continuous layer of reinforcement, which is in direct contact with the UHMWPE fibers. The later configuration enhanced stress transfer between the reinforcements and fibers. It is worth noting that our bioinspired laminates have a minimal mineral content of approximately 1%, which is substantially lower than that of the arapaima scales (40%). Achieving a mineral content of 40% in the external layers of the bioinspired laminates would double their weight in comparison to those without reinforcement. Clearly this would be problematic for industrial applications in aerospace and sports where weight reduction is always a priority.

The hierarchical approach involving the introduction of nano-scale reinforcements enabled the fabrication of high-strength composites with low-density. Both manners of reinforcement significantly increased the stiffness and energy absorption with minimal increase in weight (figure 7). While the addition of Al_2O_3 reinforcements was accompanied by a 2.5% increase in weight, the TiN reinforcement caused an increase of approximately 0.15%. Both forms of the nano-scale reinforcements served as extremely thin layers of stiff reinforcements with no significant increase in weight. Nevertheless, both forms of reinforcement interacted with the UHMWPE fibers (figure 6) and plies in a manner that improved the overall mechanical performance of the material.

A recent study concerning the deformation mechanisms of unreinforced UHMWPE composites under transverse impact reported that failure occurs in a progressive manner. Ply fracture begins at the interface between the striker and the composite and propagates to the rear of the laminate [38]. The failure process occurs through tensile failure of the plies by an indirect tension mechanism, wherein the transverse compression stresses generate tensile stresses in-plane due to a mismatch in the properties between the alternating 0° and 90° plies. This process is accompanied by fiber sliding, which is evidenced by

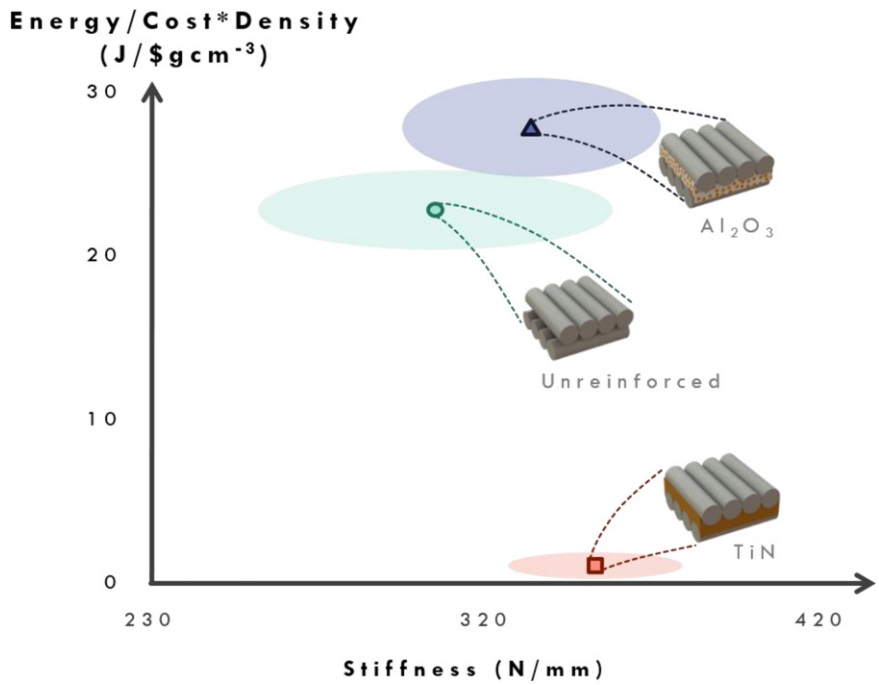

Figure 7. Figure of merit representing materials performance accounting for energy absorption, weight and manufacturing cost (energy/cost*density) as a function of the stiffness for the bioinspired and unreinforced composites. Colored areas with transparency represent the standard deviation of the measurements for each type of material.

outward extruded fibers found in the cross-section of the impacted composites. This interaction occurs at both the ply and fiber levels, which ranges across three decades of length scale (1 μm to 1 mm). However, when nano-reinforcements are integrated into the laminates, interfacial friction between the plies limits the sliding and stretching of fibers, thereby improving the coupling between fibers. Thus, in the development of tensile stresses within the fibers through indirect tension, the increased friction spreads fiber recruitment in supporting the mechanical load. That process ultimately allows the stress to be distributed over wider areas, thus reducing damage. Certainly, the increased friction between fibers is a complementary mechanism of energy dissipation facilitated by the nano-scale reinforcements, which manifests as an increase in the mechanical performance of the reinforced materials at the macro scale.

Similar phenomena have been found in both natural and artificial systems. For instance, in fish scales, dehydration causes resistance to sliding between collagen fibers, which increases the elastic modulus and strength of dehydrated scales [25, 37]. The stiffening mechanisms associated with this phenomenon have already been reported by Jiang *et al* [39]. Similarly, in synthetic systems such as liquid armor, the high-performance fabrics increase their mechanical properties via resistance to fiber sliding promoted by the introduction of shear thickening fluids (STF) [40]. STF are dense colloidal suspensions that can exhibit an abrupt increase in the viscosity with an adequate increase in shear rate or applied stresses. When used in protective applications, STF improve the performance of the fabrics, but their major contribution is not derived from their shear thickening behavior. Rather, the solid particles increase the friction between fibers, which ultimately causes spreading of the load over wider areas [41–43]. Particle volume fraction and particle size are some of the characteristics that affect the performance of STFs. These factors could also affect our bioinspired materials. The lower limit of the particle volume fraction for the thickening behavior of colloidal suspensions depends on the material properties. It has been reported that the thickening behavior of STF is generally activated at a particle volume fraction exceeding 0.5 [41]. In contrast, the volume fraction of Al_2O_3 particles in the present work was about 0.01, which is significantly lower than that stated to trigger the thickening behavior of the STF. Although impact tests show that this minimum volume fraction (0.01) can improve the energy absorption and stiffness of bioinspired laminates, future work investigating the effect of this volume fraction on the properties of the laminate is warranted, as this may open new opportunities for optimization.

An analysis of the relations between fibers and reinforcements for the natural and bioinspired materials show important similarities. The collagen fibers present in *A. gigas* scales have a diameter of 1 μm with a mineral reinforcement consisting of platelets with a thickness of 50 nm [22, 25]. On the other hand, the fibers present in our bioinspired laminates have a diameter of 17 μm accompanied by reinforcements of different sizes depending on the nano-mineralization

strategy. The Al_2O_3 particles were approximately 500 nm diameter, and the TiN reinforced layer thicknesses were approximately 300 nm. The reinforcement/fiber (RF) ratio, defined as the ratio between particle diameter (or coating thickness), and fiber diameter, shows that the arapaima scales exhibit an RF ratio of 0.05. That value for the Al_2O_3 and TiN reinforced laminates is ∼0.03 and ∼0.02, respectively. Future studies that explore the importance of this ratio between the constituent units of bioinspired laminates and their effect on internal friction could lead to further improvements on mechanical properties.

Previous studies have shown that the stacking sequence of unidirectional fiber laminates can significantly affect the mechanical behavior of bioinspired composites. Hazzard *et al* [44] showed that lamination patterns such as rotational, helicoidal or quasi-isotropic configurations can achieve superior mechanical behavior of thin Dyneema® panels under low-velocity impacts when compared with cross-ply arrangements. They suggested that the deformation mechanisms exhibited by cross-ply laminates were dominated by substantial in-plane shear with limited load transfer from primary fibers, which is an energy dissipation mechanism exhibited at the microscale (1 μm to 1 mm). The load transfer between fibers could be maximized by introducing nano-scale reinforcements following the strategy applied here. Considering that the laminates in this work were inspired by the cross-ply patterns in arapaima scales [33], further work could consider the combined effect of nano reinforcements and varying lamination patterns on the mechanical properties of the materials.

One of the primary aims of this work was to develop strategies for manufacturing hierarchical low weight energy absorption materials that could be easily adopted in the industry. The effect of the manufacturing process on energy and weight variations can be analyzed if a figure of merit relating energy absorbed, density and cost is used, as shown in figure 7. Here, an increased value will represent low weight and low cost with increased energy absorption. According to this ranking, the addition of nanoparticles stands out as a viable option for industrial scaling. Radio frequency magnetron sputtering increases the cost about 17 times in comparison to the unreinforced material, whereas the production cost of the nanoparticle reinforcements results in just about 1.3% increase. Given that no significant differences were found in the impact resistance between the two bioinspired materials, introducing reinforcements by nano-spray coating is considered the best option to be industrially scaled.

5. Concluding remarks

This work proposed a hierarchical approach to mimic the graded mineralization exhibited by arapaima scales, with a variation in the level of mineralization from the top to the bottom of elasmodine. By using two different nano mineralization strategies (i.e., Al_2O_3 nanoparticles and TiN nanocoatings) into a laminar organic fibrous composite, three different sample typologies were obtained: (i) unreinforced, (ii) reinforced with Al_2O_3, and (iii) reinforced with TiN. Dynamic tests revealed that the impact resistance of the reinforced materials was increased significantly with respect to the non-reinforced materials, with a 20%–23% increase in absorbed energy for materials reinforced with Al_2O_3 and TiN, respectively. Remarkably, this enhancement in impact performance was obtained with a negligible increase in the weight (i. e., less than 2, 5% in Al_2O_3-reinfoced materials and barely 0, 15% in TiN-reinforced materials). The microscopy analysis suggested that the enhanced impact performance resulted from a new energy dissipation mechanism at the nanoscale. This mechanism involves increased friction between the fibrous layers of the laminate through interfacial nano-scale reinforcements. Remarkably, the Al_2O_3-based mineralization strategy can be industrially scaled up due to their low added costs. Therefore, this strategy for developing bioinspired hierarchical materials may bring the benefits of biomimetics to the next generation of light-weight, cost-efficient, impact-tolerant, high-performance protective materials.

Acknowledgments

The authors like to express their gratitude to Universidad EAFIT for their financial support.

ORCID iDs

Juan Camilo Múnera https://orcid.org/0000-0001-6452-5445
Dwayne Arola https://orcid.org/0000-0001-9140-2758
Alex Ossa https://orcid.org/0000-0002-3687-9307

References

[1] Meyers M A, Chen P Y, Lopez M I, Seki Y and Lin A Y M 2011 Biological materials: a materials science approach *J. Mech. Behav. Biomed. Mater.* **4** 626–57
[2] Chen P Y, McKittrick J and Meyers M A 2012 Biological materials: functional adaptations and bioinspired designs *Prog. Mater. Sci.* **57** 1492–704
[3] Naleway S E, Porter M M, McKittrick J and Meyers M A 2015 Structural design elements in biological materials: application to bioinspiration *Adv. Mater.* **27** 5455–76
[4] Yang W, Meyers M A and Ritchie R O 2019 Structural architectures with toughening mechanisms in nature: a review of the materials science of type-I collagenous materials *Prog. Mater. Sci.* **103** 425–83
[5] Huang W, Restrepo D, Jung J, Su F Y, Liu Z, Ritchie R O, McKittrick J, Zavattieri P and Kisailus D 2019 Multiscale toughening mechanisms in biological materials and bioinspired designs *Adv. Mater.* **31** 1901561

[6] San Ha N and Lu G 2020 A review of recent research on bio-inspired structures and materials for energy absorption applications *Composites* B **181** 1–38
[7] Barthelat F 2007 Biomimetics for next generation materials *Phil. Trans. R. Soc.* A **365** 2907–19
[8] Weaver J C *et al* 2012 The stomatopod dactyl club: a formidable damage-tolerant biological hammer *Science* **336** 1275–80
[9] Rudykh S, Ortiz C and Boyce M C 2015 Flexibility and protection by design: imbricated hybrid microstructures of bio-inspired armor *Soft Matter* **11** 2547–54
[10] Valashani S M M and Barthelat F 2015 A laser-engraved glass duplicating the structure, mechanics and performance of natural nacre *Bioinsp. Biomim.* **10** 026005
[11] Mirkhalaf M, Tanguay J and Barthelat F 2016 Carving 3D architectures within glass: exploring new strategies to transform the mechanics and performance of materials *Extreme Mech. Lett.* **7** 104–13
[12] Grunenfelder L K *et al* 2014 Bio-inspired impact-resistant composites *Acta Biomater.* **10** 3997–4008
[13] Yin Z, Hannard F and Barthelat F 2019 Impact-resistant nacre-like transparent materials *Science* **364** 1260–3
[14] Gu G X, Takaffoli M and Buehler M J 2017 Hierarchically enhanced impact resistance of bioinspired composites *Adv. Mater.* **29** 1700060
[15] Miao T, Shen L, Xu Q, Flores-Johnson E A, Zhang J and Lu G 2019 Ballistic performance of bioinspired nacre-like aluminium composite plates *Composites* B **177** 107382
[16] Miranda P, Pajares A and Meyers M A 2019 Bioinspired composite segmented armour: numerical simulations *J. Mater. Res. Technol.* **8** 1274–87
[17] Ong C W R, Zhang M H, Du H and Pang S D 2019 Functionally layered cement composites against projectile impact *Int. J. Impact Eng.* **133** 103338
[18] Malik I A and Barthelat F 2016 Toughening of thin ceramic plates using bioinspired surface patterns *Int. J. Solids Struct.* **97–98** 389–99
[19] Mirkhalaf M and Barthelat F 2017 Design, 3D printing and testing of architectured materials with bistable interlocks *Extreme Mech. Lett.* **11** 1–7
[20] Meyers M A, Chen P Y, Lin A Y M and Seki Y 2008 Biological materials: structure and mechanical properties *Prog. Mater. Sci.* **53** 1–206
[21] Martini R, Balit Y and Barthelat F 2017 A comparative study of bio-inspired protective scales using 3D printing and mechanical testing *Acta Biomater.* **55** 360–72
[22] Meyers M A, Lin Y S, Olevsky E A and Chen P-Y 2012 Battle in the Amazon: Arapaima versus Piranha *Adv. Eng. Mater.* **14** B279–88
[23] Yang W, Quan H, Meyers M A and Ritchie R O 2019 Arapaima fish scale: one of the toughest flexible biological materials *Matter* **1** 1–10
[24] Yang W *et al* 2014 Protective role of *Arapaima gigas* fish scales: structure and mechanical behavior *Acta Biomater.* **10** 3599–614
[25] Lin Y S, Wei C T, Olevsky E A and Meyers M A 2011 Mechanical properties and the laminate structure of *Arapaima gigas* scales *J. Mech. Behav. Biomed. Mater.* **4** 1145–56
[26] Sherman V R, Quan H, Yang W, Ritchie R O and Meyers M A 2017 A comparative study of piscine defense: the scales of *Arapaima gigas, Latimeria chalumnae and Atractosteus spatula J. Mech. Behav. Biomed. Mater.* **73** 1–16
[27] Yang W, Quan H, Meyers M A and Ritchie R O 2019 Arapaima fish scale: one of the toughest flexible biological materials *Matter* **1** 1–10
[28] Browning A, Ortiz C and Boyce M C 2013 Mechanics of composite elasmoid fish scale assemblies and their bioinspired analogues *J. Mech. Behav. Biomed. Mater.* **19** 75–86
[29] Khayer Dastjerdi A and Barthelat F 2015 Teleost fish scales amongst the toughest collagenous materials *J. Mech. Behav. Biomed. Mater.* **52** 95–107
[30] Vernerey F J and Barthelat F 2010 On the mechanics of fishscale structures *Int. J. Solids Struct.* **47** 2268–75
[31] Zhu D, Ortega C F, Motamedi R, Szewciw L, Vernerey F and Barthelat F 2012 Structure and mechanical performance of a 'modern' fish scale *Adv. Eng. Mater.* **14** B185–94
[32] Zhu D, Szewciw L, Vernerey F and Barthelat F 2013 Puncture resistance of the scaled skin from striped bass: collective mechanisms and inspiration for new flexible armor designs *J. Mech. Behav. Biomed. Mater.* **24** 30–40
[33] Murcia S, Lavoie E, Linley T, Devaraj A, Ossa E A and Arola D 2017 The natural armors of fish: a comparison of the lamination pattern and structure of scales *J. Mech. Behav. Biomed. Mater.* **73** 17–27
[34] Zimmermann E A, Gludovatz B, Schaible E, Dave N K N, Yang W, Meyers M A and Ritchie R O 2013 Mechanical adaptability of the Bouligand-type structure in natural dermal armour *Nat. Commun.* **4** 1–7
[35] Ghods S, Murcia S, Ossa E A and Arola D 2019 Designed for resistance to puncture: the dynamic response of fish scales *J. Mech. Behav. Biomed. Mater.* **90** 451–9
[36] Arola D, Murcia S, Stossel M, Pahuja R, Linley T, Devaraj A, Ramulu M, Ossa E A and Wang J 2018 The limiting layer of fish scales: structure and properties *Acta Biomater.* **67** 319–30
[37] Murcia S, Li G, Yahyazadehfar M, Sasser M, Ossa A and Arola D 2016 Effects of polar solvents on the mechanical behavior of fish scales *Mater. Sci. Eng.* C **61** 23–31
[38] Attwood J P, Russel B P, Wadley H N and Deshpande V S 2016 Mechanisms of the penetration of ultra-high molecular weight polyethylene composite beams *Int. J. Impact Eng.* **93** 153–65
[39] Jiang H, Ghods S, Weller E, Waddell S, Ossa E A, Yang F and Arola D 2020 Contributions of intermolecular bonding and lubrication to the mechanical behavior of a natural armor *Acta Biomater.* **106** 246–55
[40] Crouch I G 2019 Body armour—new materials, new systems *Def. Technol.* **15** 241–53
[41] Gürgen S, Kuşhan M C and Li W 2017 Shear thickening fluids in protective applications: a review *Prog. Polym. Sci.* **75** 48–72
[42] Sun L L, Xiong D S and Xu C Y 2013 Application of shear thickening fluid in ultra high molecular weight polyethylene fabric *J. Appl. Polym. Sci.* **129** 1922–8
[43] Tian T, Nakano M, Li W and Li W 2018 Applications of shear thickening fluids: a review *Int. J. Hydromechatronics* **1** 238
[44] Hazzard M K, Hallett S, Curtis P T, Iannucci L and Trask R S 2017 Effect of fibre orientation on the low velocity impact response of thin Dyneema® composite laminates *Int. J. Impact Eng.* **100** 35–45